

A STUDY OF THE FOURIER-DOMAIN INTERPOLATION RECONSTRUCTION
 ALGORITHMS FOR SYNTHETIC APERTURE DIFFRACTION TOMOGRAPHY

Jian-Yu Lu

Department of Biomedical Engineering , Nanjing Institute of
 Technology , Nanjing , China

卢 建 宇

南京工学院 生物医学工程系

I. Introduction

The interpolation-free reconstruction (IFR) algorithm for synthetic aperture diffraction tomography was derived by Dr. D.Nahamoo et al.in 1984⁽¹⁾.Its datum acquisition geometry is shown in Fig.1.The transmitter and the receiver can be moved in N equal-interval sites along the line L_t and the line L_r , respectively.For every fixed position of the transmitter,the receiver can be moved in the N sites.Thus, $N \times N$ diffracted data can be obtained by using this datum acquisition geometry.

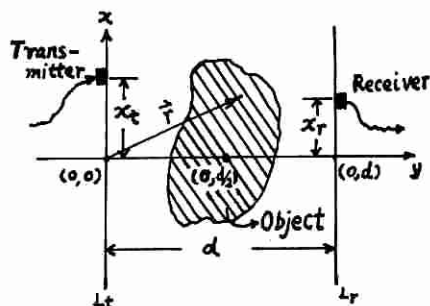


Fig.1 The datum acquisition system

The IFR algorithm requires approximately $N^3 + N^2 \log_2 N$ time

complex multiplications for an NxN image reconstructed from NxN diffracted data, therefore, it is very time-consuming. In order to save the computational time, we derived the Fourier-domain interpolation reconstruction (FDIR) algorithm which required only approximately $N^2 \log_2 N$ time complex multiplications. In addition, a computer simulation was carried out for both the IFR and the FDIR algorithms.

II. Basic Principle of the FDIR Algorithm

Applying Born approximation to the inversion of the Helmholtz equation, one can obtain the following two diffraction projection formulas⁽¹⁾

$$\tilde{F}(\vec{W}) \Big|_{\vec{W}=\vec{\lambda}-\vec{k}} = - \frac{2j\beta e^{-j\beta d}}{A_r(\alpha) A_t(k_x)} \tilde{P}_{sa}(\alpha; k_x) \quad (1)$$

and

$$\tilde{F}(\vec{W}) \Big|_{\vec{W}=\vec{Q}^{-1}(\vec{\lambda}-\vec{k})} = - \frac{2j\beta e^{-j\beta d}}{A_r(\alpha) A_t(k_x)} \tilde{P}_{sb}(\alpha; k_x) \quad (2)$$

where $\tilde{F}(\vec{W})$ is the Fourier-transform representations of $F(\vec{r})$ and $\vec{W}=(u,v)$ is a vector on the spacial frequency domain; $\vec{\lambda}=(\alpha, \beta)$ and $\vec{k}=(k_x, k_y)$, where $\beta = \sqrt{k_0^2 - \alpha^2}$ and $k_y = \sqrt{k_0^2 - k_x^2}$ ($|\alpha| \leq k_0, |k_x| \leq k_0$); $Q^{-1} = \begin{bmatrix} 0 & -1 \\ 1 & 0 \end{bmatrix}$ is a 90° rotation matrix; $\tilde{P}_{sa}(\alpha; k_x)$ and $\tilde{P}_{sb}(\alpha; k_x)$ are the Fourier transforms of the diffracted data before and after 90° counterclockwise rotation of the object around the point $(0, d/2)$, respectively; $A_r(\alpha)$ and $A_t(k_x)$ are the functions which relate to the characteristics of the transmitter and the receiver respectively; and d is the distance between the two lines L_t and L_r , as shown in Fig.1.

In order to obtain $F(\vec{r})$ from $\tilde{F}(\vec{W})$ by using the inverse fast Fourier transform (IFFT), we must find the values of $\tilde{F}(\vec{W})$ on the rectangular grids. For that purpose, we have derived the following relationships which relate the rectangular coordinates to the curvilinear coordinates

$$\begin{cases} \alpha = \frac{1}{2} (u - \sigma_1) \\ k_x = -\frac{1}{2} (u + \sigma_1) \end{cases} \text{ when } u \cdot v \geq 0, \text{ or } \begin{cases} \alpha = \frac{1}{2} (u + \sigma_1) \\ k_x = -\frac{1}{2} (u - \sigma_1) \end{cases} \text{ when } u \cdot v < 0 \quad (3)$$

where

$$\sigma_1 = |v| \cdot \sqrt{\frac{4 k_0^2}{u^2 + v^2} - 1} \quad (4)$$

for all the points $\vec{W}=(u,v)$ belong to the region $\{|\vec{\lambda}-\vec{K}|/(|\alpha|\leq k_0, |k_x|\leq k_0)\}$ and

$$\begin{cases} \alpha = -\frac{1}{2}(v-\sigma_2) \\ k_x = \frac{1}{2}(v+\sigma_2) \end{cases} \text{ when } u \cdot v \geq 0, \text{ or } \begin{cases} \alpha = -\frac{1}{2}(v+\sigma_2) \\ k_x = \frac{1}{2}(v-\sigma_2) \end{cases} \text{ when } u \cdot v < 0 \quad (5)$$

where

$$\sigma_2 = |u| \cdot \sqrt{\frac{4k_0^2}{u^2 + v^2} - 1} \quad (6)$$

for all the points $\vec{W}=(u,v)$ belong to the region $\{Q^{-1}(\vec{\lambda}-\vec{K})/(|\alpha|\leq k_0, |k_x|\leq k_0)\}$.

From the relationships above, we will find the point $(\alpha; k_x)$ on the curvilinear coordinates from a given grid point (u,v) , and then, using the bilinear or other interpolation methods⁽⁴⁾, we will find the value of $\tilde{F}(\vec{W})$ on this point from the known values of $\tilde{F}(\vec{W})$ on the discrete points $(\alpha_i; k_{xj})$ (Because only $N \times N$ diffracted data are available, $\tilde{F}(\vec{W})$ in Eqs.(1) and (2) is known on $N \times N$ discrete points $(\alpha_i; k_{xj})$ on the curvilinear coordinates), where $i, j=1, \dots, N$. By multiplying $\tilde{F}(\vec{W})$ with a proper window and using IFFT, we will obtain the image function $F(\vec{r})$.

III. Results and Conclusion

Fig.2 is a head phantom used in our computer simulations. It is as the same phantom as used by Shepp and Logan⁽²⁾ except that the gray levels are changed to those used by Devaney⁽³⁾ and Pan and Kak⁽⁴⁾.

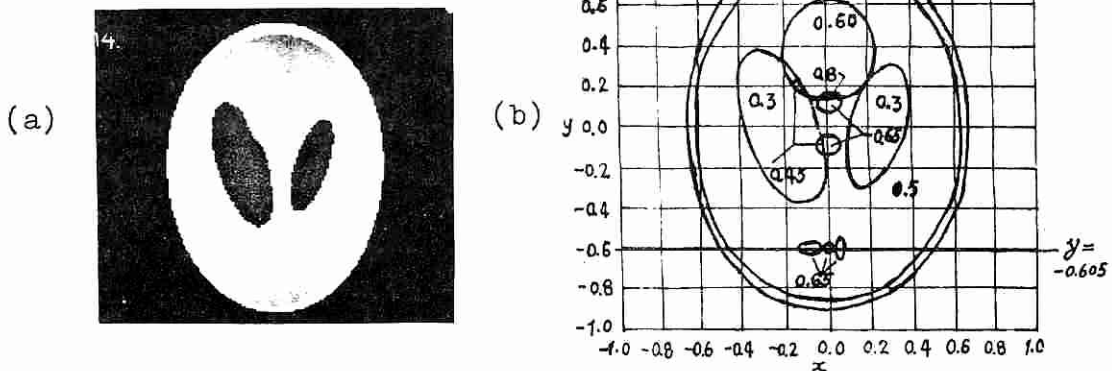


Fig.2 The head phantom used in our computer simulations
 (a) A photograph of the phantom (b) Numerical gray-level assignments of the phantom

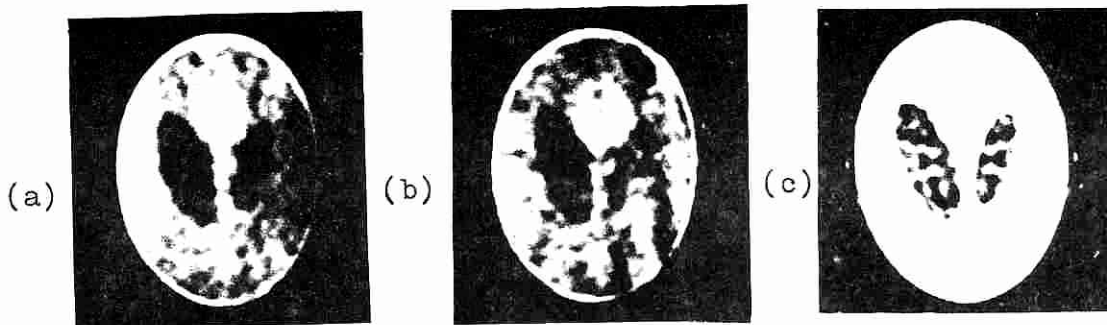


Fig.3 128x128 pixel images reconstructed from 128x128 diffracted data by using the bilinear interpolation (a), the nearest-neighbor interpolation (b) and the interpolation-free reconstruction algorithm (c).

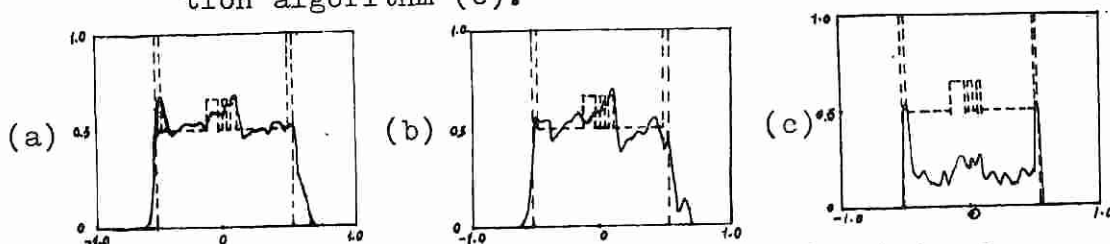


Fig.4 The comparisons between the reconstructed values (real lines) and the real values (dash lines) along the line $y=-0.605$ (refer to Fig.2). (a), (b) and (c) are corresponding to those shown in Fig.3

The results of our computer simulations are shown in Fig. 3 and Fig.4. Fig.3 contains the images reconstructed from the FDIR and the IFR algorithms. Fig.4 shows the comparisons of the reconstructed values and the real values along the line $y=-0.605$ (refer to Fig.2 (b)).

From the photographs shown in the above, one can see that the image reconstructed by the bilinear interpolation reconstruction algorithm has less artifacts. This fact can also be seen from the figures of the reconstructed values. Therefore, we can conclude that the bilinear interpolation reconstruction algorithm gives the best results.

Acknowledgement

The author is grateful to Prof. Yu Wei, the author's supervisor, for her help in this work.

References

1. D.Nahamoo, S,X.Pan and A.C.Kak: IEEE Trans.Son.& Ultrason. 31, 4(1984)
2. L.A.Shepp and B.F.Logan: IEEE Trans. Nucl. Sci. 21, (1974)
3. A.J.Devaney: Ultrason. Imag. 4, (1982)
4. S.X.Pan and A.C.Kak: IEEE Trans. ASSP. 31, (1983)